European Journal of Pharmaceutical Sciences 44 (2011) 288–298

Contents lists available at SciVerse ScienceDirect

European Journal of Pharmaceutical Sciences

journal homepage: www.elsevier.com/locate/ejps

Mathematical modeling of drug delivery from one-layer and two-layer torus-shaped devices with external mass transfer resistance

Ignacio M. Helbling *, María I. Cabrera, Julio A. Luna

Laboratorio de Química Fina, Instituto de Desarrollo Tecnológico para la Industria Química (INTEC), Universidad Nacional del Litoral and Consejo Nacional de Investigaciones Científicas y Técnicas (UNL-CONICET), CCT CONICET-SANTA FE, Ruta Nacional 168, Paraje El Pozo, 3000 Santa Fe, Argentina

ARTICLE INFO

Article history:
Received 23 May 2011
Received in revised form 15 July 2011
Accepted 9 August 2011
Available online 16 August 2011

Keywords:
Vaginal ring
Pseudo-steady state approximation
Mass transfer resistance
Mathematical modeling
Moving front
Drug delivery

ABSTRACT

A mathematical modeling of controlled release of drug from one-layer and two-layer torus-shaped devices with external mass transfer resistance is presented. Analytical solutions based on the pseudo-steady state approximation are derived. The validity of the equations is established in two stages. In the first stage, the validity of the models derived for more complex systems is determined by comparison with profiles predicted by the simplest model, in asymptotic cases. In the second stage, the reliability and usefulness of the models are ascertained by comparison of the simulation results with vaginal rings experimental release data reported in the literature. In order to measures quantitatively the fit of the theoretical models to the experimental data, the pair-wise procedure is used. A good agreement between the prediction of the models and the experimental data is observed. The models are applicable only to torus-shaped systems in where the initial load of drug is higher than its solubility in the polymer.

1. Introduction

Drug delivery is an important aspect of medical treatment. The efficacy of many drugs is directly related to the way in which they are administered. Some therapies require that the drug be repeatedly administered to the patient over a long period of time. This presents certain drawbacks. For contraception, for example, daily oral intake of pills increases the risk of forgetting the intake. In addition, the hepatic first-pass reduces the bioavailability of the drug. Therefore, new routes of administration have been explored.

The administration of drug by the vagina has been described and the advantages of this via over oral administration have been noted (Cicinelli, 2008; Hussain and Ahsan, 2005). The vagina appears as an interesting route of drug administration for treatment not only local but also for systemic (Cicinelli, 2008; Hussain and Ahsan, 2005). Controlled release devices for vaginally drug delivery have been explored (Sitruk-Ware, 2006; Yoo and Lee, 2006). Among others, the intravaginal rings (IVRs) appear to be the most promising devices and have been used extensively. Several designs of ring have been developed, including matrix, reservoir and shell-type variants, each providing very different drug release profiles (Malcolm et al., 2002, 2003a; Woolfson et al., 1999, 2003). Despite a substantial body of work has been published to date on the development, implementation and clinical trials of IVRs (Johansson and Sitruk-Ware, 2004; Malcolm et al., 2003b; Roumen, 2008; Van Laarhoven et al., 2002), no attempt has been made to derive a model for predicting drug release rates.

In the past, different strategies have been used to model the drug release kinetic in systems with different geometric shapes (Arifin et al., 2006; Helbling et al., 2010a; Siepmann et al., 2008; Wu and Brazel, 2008). One of the most used has been the application of the approach of pseudo-steady state. The pseudo-steady state approximation (PSSA) was introduced first by Higuchi to derive an analytical solution for a rectangular slab under "sink condition" (Higuchi, 1961, 1963). Since then, this approach was used by many authors for the derivation of mathematical models. For example, Roseman and Higuchi (1970) and Tojo (1985) assumed PSSA in the modeling of a planar geometry device with the existence of a stagnant liquid layer. The same analysis but incorporating a finite external medium was carried out by Zhou and Wu, who derived an explicit analytical solution assuming PSSA (Zhou and Wu, 2002). Helbling et al. derived analytical solutions based on PSSA for the release of drug from erodible and non-erodible planar matrices, through a membrane, and taking into account the existence of a diffusion boundary layer and a finite release medium (Helbling et al., 2010b). In other systems, like cylinder or spheres, also PSSA was employed to develop the predicting equation to adjust the release data (Costa and Sousa Lobo, 2003; Roseman, 1972; Siepmann and Siepmann, 2008; Zhou and Wu, 2003).

In our previous work (Helbling et al., 2011), a mathematical model to predict the release of drug from torus-shaped one-layer

* Corresponding author. Tel./fax: +54 342 4511597.
E-mail address: ihelbling@santafe-conicet.gov.ar (I.M. Helbling).

0928-0987/$ - see front matter © 2011 Elsevier B.V. All rights reserved.
doi:10.1016/j.ejps.2011.08.008

Nomenclature

a_{dis}	area of the interface of the dispersed-drug zone/depleted drug zone (cm^2)
a_{rel}	release area of the device (cm^2)
A	initial drug loading in the device (mg/cm^3)
$C_{a,1}$	dissolved-drug concentration in the external resistance layer at the matrix-external resistance layer interface (mg/cm^3)
$C_{a,2}$	dissolved-drug concentration in the external resistance layer at the membrane-external resistance layer interface (mg/cm^3)
C_{bl}	dissolved-drug concentration in the external resistance layer (mg/cm^3)
$C_{eq,1}$	dissolved-drug concentration in matrix at the matrix-external resistance layer interface (mg/cm^3)
$C_{eq,2}$	dissolved-drug concentration in matrix at the matrix-membrane interface (mg/cm^3)
C_m	dissolved-drug concentration in the membrane (mg/cm^3)
$C_{m,1}$	dissolved-drug concentration in the membrane at the matrix-membrane interface (mg/cm^3)
$C_{m,2}$	dissolved-drug concentration in the membrane at the membrane-external resistance layer interface (mg/cm^3)
C_s	maximum drug solubility in the polymeric matrix (mg/cm^3)
C_t	dissolved-drug concentration in the matrix (mg/cm^3)
D_a	drug diffusion coefficient in the external resistance layer (cm^2/s)
D_m	drug diffusion coefficient in the membrane (cm^2/s)
D_p	drug diffusion coefficient in the polymeric matrix (cm^2/s)
h_a	thickness of the external resistance layer (cm)
h_m	thickness of the membrane (cm)
K_1	drug partition coefficient at the matrix-external resistance layer interface (dimensionless)
K_2	drug partition coefficient at the matrix-membrane interface (dimensionless)
K_3	drug partition coefficient at the membrane-external resistance layer interface (dimensionless)
m	cumulative amount of drug released (mg)
Q	cumulative amount of drug released per unit area of the device (mg/cm^2)
r	spatial coordinates (cm)
R_e	distance from the rotation axis to the external surface of the matrix (cm)
R_g	distance from the rotation axis to the center of the generating circle (cm)
R_0	radius of the generating circle (cm)
$S(t)$	position of the dissolution–diffusion moving front (cm)
t	time (s)
V_s	volume of the torus-shaped matrix (cm^3)

Greek letters

$\delta(t)$	position of the dissolution–diffusion moving front (dimensionless)

devices with initial drug loading higher than the maximum solubility of drug in the polymer, assuming PSSA and taking into account the specific characteristic of the torus-shaped geometry on the release process was developed. This model showed to be efficient in the prediction of the profiles of drug released. Based on these results, the need for a model that includes other effects such as the presence of resistance to mass transfer is a fact.

The purpose of the present study was to extend the analysis previously done by developing a model that takes into account the presence of external mass transfer resistance. Also, a model that predicts the release profiles from a torus-shaped two-layer device is derived. The new models were derived based on PSSA and can cover a wider range of situations.

2. Model development

The mathematical model is developed for a torus-shaped device containing solid drug particles. The device is schematically illustrated in Fig. 1. When the torus-shaped device is placed in the release medium, the liquid takes contact with the device over its entire surface. As the liquid contacts the device, the solid drug particles dissolve in and then diffuse out of the matrix. The discrete crystals in the layer closer to the matrix surface are the first to elute. When this layer becomes "exhausted", the solid drugs in the next layer begin to be depleted. So, a drug depletion zone is created. The thickness of this zone increases with time and as more solid drugs elute out of the device, thus leading to the inward advancement of the interface of the dispersed-drug zone/depleted drug zone, phenomenon commonly referred to as "dissolution–diffusion moving front". Because the liquid comes in contact with the device over its entire surface at the same time, the formation of the depletion zone and therefore the inward advancement of the interface of the dispersed-drug zone/depleted drug zone takes place in all radial directions at the same time (considering a radial direction as the direction of the radius of the generating circle for a particular value of φ) (Helbling et al., 2011). This means that the same phenomenon of "dissolution–diffusion moving front" takes place for all value of φ (from 0 to 2π) and also for any value of ω (from 0 to 2π) (Helbling et al., 2011). So, it is sufficient to find the way in which the front moves in a single radial direction and then extrapolated it to the entire device, since the front moves in the same form in all the radial directions. Therefore, for the mathematical analysis only the half section of the area of the generating circle in the radial direction $\varphi = 0$ ($R_g < r < R_e$) and in a particular value of ω (the value of ω is irrelevant because the same phenomenon occurs for all ω) is considered. The analysis can be then extrapolated to the entire device (Helbling et al., 2011). The parameters present in Fig. 1 are defined below.

The general assumptions of the model to be mathematically formulated are the following: (i) The system is a torus-shaped device. (ii) The device is considered as an isotropic medium. (iii) The device is composed by a polymeric matrix that contains solid drug particles dispersed in its interior. (iv) The initial distribution of the drug in the polymeric matrix is homogeneous. (v) The initial drug loading in the matrix is higher than the maximum drug solubility in the polymer. (vi) For simplicity, all the drug particles have the same size and a spherical form. (vii) The polymeric matrix is inert, unswellable and non-erodible. (viii) For a one-layer device, the system consists only of a polymeric matrix. In the case of a two-layer device, the system consists of the polymeric matrix coated with a second empty layer that resembles a membrane. (ix) The initial drug loading in the membrane is zero. (x) The membrane is inert, unswellable and non-erodible. (xi) The membrane can be made up of the same polymer as the matrix or of a different one. (xii) When the "dissolution–diffusion moving front" begins to move, the dissolved drug profile is attained instantaneously

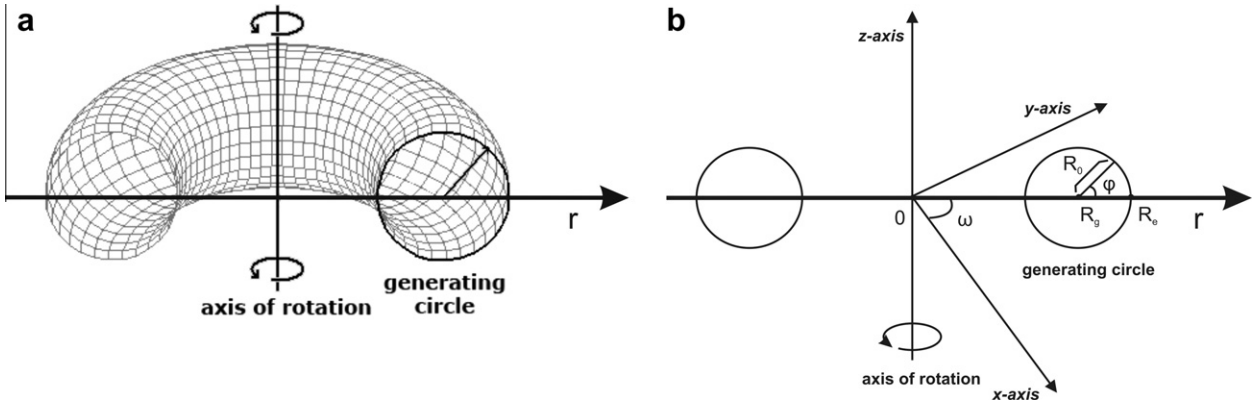

Fig. 1. Schematic illustration of a torus. (a) Construction of a torus. (b) Schematic representation of a torus in cartesian coordinate system.

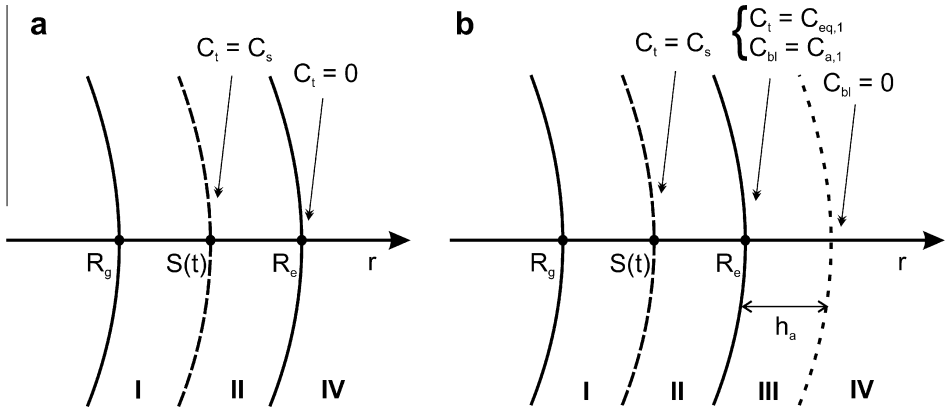

Fig. 2. Schematic illustration of the dissolved-drug concentration profile in the considered section of the torus-shaped one-layer device. (a) Without external resistance layer. (b) With external resistance layer. (I) Dispersed-drug zone; (II) dissolved-drug zone; (III) stagnant liquid layer; and (IV) infinite release medium.

throughout the thickness of the membrane. (xiii) The dissolution of the solid drug particles in the polymeric matrix occurs at a high rate and does not constitute a controlling step of the general release process. (xiv) The rate controlling step of the release process is the drug diffusion across the polymeric matrix in the one-layer device or across the membrane in the two-layer device, which are described according to Fick's laws. (xv) The mass transport of drug is assumed to be radial at all points. (xvi) The drug diffusion coefficient in the polymeric matrix and in the membrane are considered constant. (xvii) The pseudo steady-state approximation (PSSA) is assumed during the whole modeling process. (xviii) External resistance to mass transfer is not negligible. (xix) The drug diffusion coefficient in the external resistance layer is considered constant. (xx) The initial drug concentration in the external resistance layer is zero. (xxi) The volume of the release medium is considered infinite compared with the device to ensure the "sink" condition. (xxii) For a given time t, there exist a drug depletion zone with a thickness $R_e - S(t)$. (xxiii) The model formulated is valid till all solid drug particles dissolve in the polymer and no discrete crystals remains in the device. This stage is achieved when the "dissolution–diffusion moving front" reaches $r = R_g$. (xxiv) At the initial time ($t = 0$), the elution medium has not been yet in contact with the dispersed drug and therefore there is no depletion zone. It is considered that the "dissolution–diffusion moving front" is at the surface of the matrix ($S = R_e$) at the initial time. In the case of a two-layer device, the time required for the diffusion of the elution medium through the membrane is very short and can be neglected.

2.1. One-layer device

The dissolved-drug concentration profile in the considered section of the torus-shaped one-layer device is illustrated in Fig. 2. Fig. 2a corresponds to a system without external resistance and the mathematical analysis was discussed in our previous work (Helbling et al., 2011). Fig. 2b corresponds to a system that has an external layer that acts as a resistance to mass transfer. The device is composed by a polymeric matrix that contains solid drug particles dispersed in its interior. The drug release is controlled by the diffusion of drug through the matrix. There is no additional internal resistance to mass transfer that the diffusion of drug through the polymeric matrix in these devices. The presence of the external resistance layer depends on the conditions under which the in vitro release test is performed. Chien reported about the dependency of stagnant liquid layer with the viscosity, drug diffusion coefficient and agitation speed of the release medium (Chien, 1982). For example, low stirring speed of the release medium leads to the formation of a stagnant liquid layer that acts as an external resistance to mass transfer (Chien, 1982).

The parameters present in Fig. 2 are: r is the spatial coordinates, R_g is the distance from the rotation axis to the center of the generating circle, $S(t)$ is the position of the "dissolution–diffusion moving fronts", R_e is the distance from the rotation axis to the external surface of the matrix, h_a is the thickness of the external resistance layer, C_t is the dissolved-drug concentration in the matrix, C_s is the maximum solubility of drug in the polymeric matrix, $C_{eq,1}$ is the dissolved-drug concentration in matrix at the matrix-

external resistance layer interface, C_{bl} is the dissolved-drug concentration in the external resistance layer and $C_{a,1}$ is the dissolved-drug concentration in the external resistance layer at the matrix-external resistance layer interface.

The equation of heat-conduction in a general orthogonal curvilinear coordinate system was reported by Özişik (1980). It is known that there is an analogy between the heat-conduction process and the diffusion process (Crank, 1975). This was recognized by Fick, who first put diffusion on a quantitative basis by adopting the mathematical equation of heat-conduction (Fick, 1855). So, the equation reported by Özişik can be employed for diffusion problems. The first stage in the mathematical modeling of this system is to determine the concentration profile of dissolved-drug in the depletion zone formed inside the matrix. For torus-shaped device with solute diffusion being radial at all points, the governing equation for diffusion in the depletion zone is (Helbling et al., 2011):

$$\frac{\partial C_t}{\partial t} = \frac{D_p}{r(R_g+r)}\frac{\partial}{\partial r}\left(r(R_g+r)\frac{\partial C_t}{\partial r}\right) \quad t>0 \quad S(t)\leqslant r\leqslant R_e \tag{1}$$

where t is the time and D_p is the drug diffusion coefficient in the polymeric matrix. Assuming equilibrium between the surface of the device and the external fluid at all t, the initial and boundary conditions are:

$$C_t = C_s \quad t=0 \quad R_g\leqslant r\leqslant R_e \tag{2}$$

$$C_t = C_s \quad t>0 \quad R_g\leqslant r\leqslant S(t) \tag{3}$$

$$C_t = C_{eq,1} \quad t>0 \quad r=R_e \tag{4}$$

With $\partial C_t/\partial t$ in Eq. (1) being fixed at zero according to the PSSA and with the boundary conditions presented in Eqs. (2)–(4), the concentration distribution of dissolved-drug in the depletion zone can be derived as:

$$C_t = C_s\left[1-\left(1-\frac{C_{eq,1}}{C_s}\right)\frac{\ln\left(\frac{(R_g+S)r}{S(R_g+r)}\right)}{\ln\left(\frac{(R_g+S)R_e}{S(R_g+R_e)}\right)}\right] \quad t>0 \quad S(t)\leqslant r\leqslant R_e \tag{5}$$

To use the Eq. (5), the expression for $C_{eq,1}$ must be determined. This goal can be done using the concentration distribution of dissolved-drug in the external resistance layer (see Appendix A).

At the interface of the dispersed-drug zone/depleted drug zone, the following mass balance equation must be satisfied (Helbling et al., 2011):

$$-a_{dis}(A-C_s)\frac{\partial S}{\partial t} = -a_{rel}D_p\left.\frac{\partial C_t}{\partial r}\right|_{r=S(t)} \tag{6}$$

where a_{dis} is the area where the dissolution process occurs (area of the interface of the dispersed-drug zone/depleted drug zone), A is the initial drug loading in the device and a_{rel} is the release area of the device. Substituting Eq. (5) into Eq. (6), differentiating with respect to the spatial coordinates and integrating within the time lapse corresponding to the moving front between $[R_e, S]$, it yields:

$$\begin{aligned}&\frac{R_e(R_g+R_e)-S(R_g+S)}{6}+\frac{R_g^2}{6}\ln\left(\frac{R_g+S}{R_g+R_e}\right)\\&-\left(\frac{S^3}{3R_g}+\frac{S^2}{2}\right)\ln\left(\frac{(R_g+S)R_e}{S(R_g+R_e)}\right)+\frac{D_p}{D_aK_1}\ln\left(\frac{(R_g+R_e)(R_e+h_a)}{R_e(R_g+R_e+h_a)}\right)\\&\times\left(\frac{(R_e^3-S^3)}{3R_g}+\frac{(R_e^2-S^2)}{2}\right)=\frac{D_pt}{\left(\frac{A}{C_s}-1\right)}\end{aligned} \tag{7}$$

where D_a is the drug diffusion coefficient in the external resistance layer and K_1 is the drug partition coefficient at the matrix-external resistance layer interface.

The position of the "dissolution–diffusion moving front" (S) can be obtained from Eq. (7) using an adequate computational software that finds zeros of a function of one variable. The cumulative amount of solute released (m) in a given time is calculated from a mass balance equation (Helbling et al., 2011):

$$m = 2\pi^2R_g\left[A\left(R_0^2-(S-R_g)^2\right)-2\int_S^{R_e}C_t(r-R_g)\partial r\right] \tag{8}$$

where R_0 is the radius of the generating circle. Introducing Eq. (5) into Eq. (8) and integrating with respect to the spatial coordinates results in:

$$\begin{aligned}m=&2\pi^2R_g\left[A\left(R_0^2-(S-R_g)^2\right)-C_{eq,1}R_e(R_e-2R_g)\right.\\&\left.+\frac{C_sS(S-2R_g)\ln\left(\frac{(R_g+S)R_e}{S(R_g+R_e)}\right)-(C_s-C_{eq,1})\left(R_g(R_e-S)+3R_g^2\ln\left(\frac{R_g+S}{R_g+R_e}\right)\right)}{\ln\left(\frac{(R_g+S)R_e}{S(R_g+R_e)}\right)}\right]\end{aligned} \tag{9}$$

The cumulative amount of drug release in a given time can be calculated from Eq. (9) for the case of a system in which is present an external layer that acts as a resistance to mass transfer.

2.2. Two-layer device

The dissolved-drug concentration profile in the considered section of the torus-shaped two-layer device is illustrated in Fig. 3. Fig. 3a corresponds to a system without external resistance and Fig. 3b corresponds to a system that has an external layer that acts as a resistance to mass transfer. The devices are composed in principle by two layers: the interior layer formed by a polymeric matrix that contains solid drug particles dispersed in its interior (similar to the one-layer device) and a second layer which is a polymeric membrane that has no drugs inside. The drug release from these devices is controlled by the diffusion of drug through the polymeric coating. Again, the presence of the external resistance layer depends on the condition of the release assay (Chien, 1982).

The new parameters present in Fig. 3 are: h_m is the thickness of the membrane, $C_{eq,2}$ is the dissolved-drug concentration in matrix at the matrix-membrane interface, C_m is the dissolved-drug concentration in the membrane, $C_{m,1}$ is the dissolved-drug concentration in the membrane at the matrix-membrane interface, $C_{m,2}$ is the dissolved-drug concentration in the membrane at the membrane-external resistance layer interface and $C_{a,2}$ is the dissolved-drug concentration in the external resistance layer at the membrane-external resistance layer interface.

As in the previous section, the first stage is to determine the concentration profile of dissolved-drug in the depletion zone formed inside the matrix. The governing differential equation for diffusion in the depletion zone and the associated initial and boundary conditions consist again of Eqs. (1)–(3) and the following condition (which replaces the Eq. (4)):

$$C_t = C_{eq,2} \quad t>0 \quad r=R_e \tag{10}$$

Using the same procedure as in Section 2.1, the concentration distribution of dissolved-drug in the depletion zone is given by:

$$C_t = C_s\left[1-\left(1-\frac{C_{eq,2}}{C_s}\right)\frac{\ln\left(\frac{(R_g+S)r}{S(R_g+r)}\right)}{\ln\left(\frac{(R_g+S)R_e}{S(R_g+R_e)}\right)}\right] \quad t>0 \quad S(t)\leqslant r\leqslant R_e \tag{11}$$

To use the Eq. (11), the expression for $C_{eq,2}$ must be determined. This goal can be done using the concentration distribution of dissolved-drug in the membrane (see Appendix B).

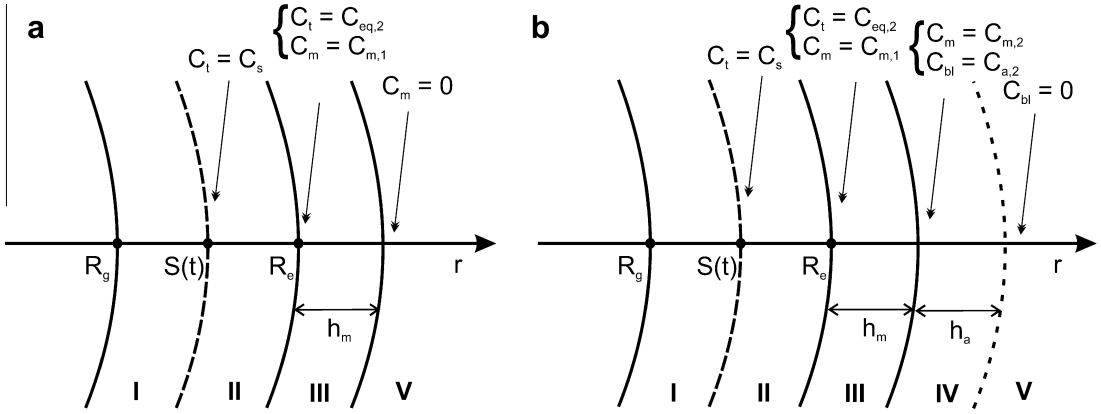

Fig. 3. Schematic illustration of the dissolved-drug concentration profile in the considered section of the torus-shaped two-layer device. (a) Without external resistance layer. (b) With external resistance layer. (I) Dispersed-drug zone; (II) dissolved-drug zone; (III) membrane; (IV) stagnant liquid layer; and (V) infinite release medium.

At the interface of the dispersed-drug zone/depleted drug zone, the mass balance given by Eq. (6) must be satisfied. Substituting Eq. (11) into Eq. (6), using Eq. (B.12a) or (B.12b), differentiating with respect to the spatial coordinates and integrating within the time lapse corresponding to the moving front between $[R_e, S]$, it yields:

$$\frac{R_e(R_g+R_e)-S(R_g+S)}{6}+\frac{R_g^2}{6}\ln\left(\frac{R_g+S}{R_g+R_e}\right)-\left(\frac{S^3}{3R_g}+\frac{S^2}{2}\right)\ln\left(\frac{(R_g+S)R_e}{S(R_g+R_e)}\right)+\frac{D_p}{D_mK_2}\ln\left(\frac{(R_g+R_e)(R_e+h_m)}{R_e(R_g+R_e+h_m)}\right)\times\left(\frac{(R_e^3-S^3)}{3R_g}+\frac{(R_e^2-S^2)}{2}\right)=\frac{D_pt}{\left(\frac{A}{C_s}-1\right)} \quad (12.a)$$

$$\frac{R_e(R_g+R_e)-S(R_g+S)}{6}+\frac{R_g^2}{6}\ln\left(\frac{R_g+S}{R_g+R_e}\right)-\left(\frac{S^3}{3R_g}+\frac{S^2}{2}\right)\ln\left(\frac{(R_g+S)R_e}{S(R_g+R_e)}\right)+\frac{D_p}{D_mK_2}\ln\left(\frac{(R_g+R_e)(R_e+h_m)}{R_e(R_g+R_e+h_m)}\right)\times\left(\frac{(R_e^3-S^3)}{3R_g}+\frac{(R_e^2-S^2)}{2}\right)\left(\frac{D_mG_2}{D_aK_3}+1\right)=\frac{D_pt}{\left(\frac{A}{C_s}-1\right)} \quad (12.b)$$

where D_m is the drug diffusion coefficient in the membrane, K_2 is the drug partition coefficient at the matrix-membrane interface and K_3 is the drug partition coefficient at the membrane-external resistance layer interface. The nomenclature presented in Eq. (12) is used throughout this section: the equations with subscript "a" in the equations number correspond to the system without external resistance layer illustrated in Fig. 3a while those having subscript "b" correspond to the system with external resistance layer illustrated in Fig. 3b. The position of the "dissolution–diffusion moving front" (S) can be obtained from Eq. (12.a) or (12.b) using an adequate computational software. The cumulative amount of solute released (m) in a given time is calculated from a mass balance equation:

$$m=2\pi^2R_g\left[A(R_0^2-(S-R_g)^2)-2\int_S^{R_e}C_t(r-R_g)\partial r-2\int_{R_e}^{R_e+h_m}C_m(r-R_g)\partial r\right] \quad (13)$$

Introducing Eq. (11), (B.5a) or (B.5b) into Eq. (13) and integrating with respect to the spatial coordinates results in:

$$m=2\pi^2R_g\left[A(R_0^2-(S-R_g)^2)+\frac{C_sS(S-2R_g)\ln\left(\frac{(R_g+S)R_e}{S(R_g+R_e)}\right)-(C_s-C_{eq,2})\left(R_g(R_e-S)+3R_g^2\ln\left(\frac{R_g+S}{R_g+R_e}\right)\right)}{\ln\left(\frac{(R_g+S)R_e}{S(R_g+R_e)}\right)}-C_{eq,2}R_e(R_e-2R_g)(1-K_2)-\frac{C_{eq,2}K_2(R_gh_m+3R_g^2\ln\left(\frac{R_g+R_e}{R_g+R_e+h_m}\right))}{\ln\left(\frac{(R_g+R_e)(R_e+h_m)}{R_e(R_g+R_e+h_m)}\right)}\right] \quad (14.a)$$

$$m=2\pi^2R_g\left[A(R_0^2-(S-R_g)^2)+\frac{C_sS(S-2R_g)\ln\left(\frac{(R_g+S)R_e}{S(R_g+R_e)}\right)-(C_s-C_{eq,2})(R_g(R_e-S)+3R_g^2\ln\left(\frac{R_g+S}{R_g+R_e}\right))}{\ln\left(\frac{(R_g+S)R_e}{S(R_g+R_e)}\right)}-C_{eq,2}R_e(R_e-2R_g)(1-K_2)-\frac{(C_{eq,2}K_2-C_{m,2})(R_gh_m+3R_g^2\ln\left(\frac{R_g+R_e}{R_g+R_e+h_m}\right))}{\ln\left(\frac{(R_g+R_e)(R_e+h_m)}{R_e(R_g+R_e+h_m)}\right)}-C_{m,2}(R_e+h_m)(R_e+h_m-2R_g)\right] \quad (14.b)$$

The cumulative amount of drug release in a given time can be calculated from Eq. (14.a) or (14.b) for the case of a two-layer device without or with external resistance layer, respectively.

3. Results and discussion

In order to use the developed models to predict the drug release profiles, it is convenient to use suitable computational programs to simplify the calculations (for example MATLAB®, FORTRAN® or MAPLE®). These programs allow the creation of a "routine" in programming language to perform the simulations. Once the routine is created, the user only needs to load the values of the parameters that make up the model and then run the program. In the present work, all the simulations were performed in the computational software MATLAB®.

To validate the models, the validation process was divided into two stages: the first stage consisted in the analysis and comparison of the behavior of the equations in asymptotic cases and the second one was to verify the ability of the models to predict real experimental drug release profiles.

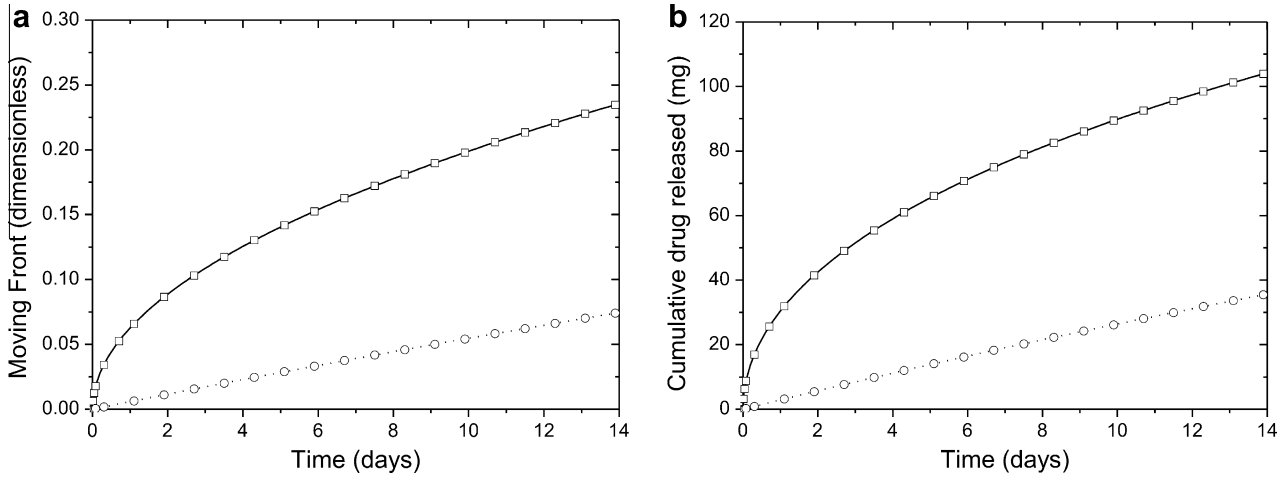

Fig. 4. Comparison of the equations behavior in absence of external resistance layer: (a) (—) model reported by Helbling et al. (2011), (□) Eq. (7), (···) Eq. (12.a) and (○) Eq. (12.b). (b) (—) model reported by Helbling et al. (2011)), (□) Eq. (9), (···) Eq. (14.a) and (○) Eq. (14.b). The parameters used are: $A/C_s = 50$; $R_e = 3.15$ cm; $R_g = 2.85$ cm; $R_0 = 0.30$ cm; $D_p = 1 \times 10^{-7}$ cm^2/s; $h_m = 0.01$ cm; $D_m = 0.5 \times 10^{-7}$ cm^2/s; $K_2 = 0.2$; $h_a = 0$.

3.1. Comparisons of asymptotic cases

For asymptotic cases means situations in which the systems are taken to a limit. In this work the limit situation was to simplify the model as much as possible. Consequently, for this stage of validation, two extreme situations were considered for the comparison of the models behavior. The first analysis was to compare the position of the "dissolution–diffusion moving front" and the cumulative amount of solute released for both, one-layer and two-layer devices, taking as condition the absence of an external resistance layer. For the one-layer device, the theoretical prediction of Eq. (7) was compared with the model previously reported by Helbling et al. (2011). For the two-layer device, the behaviors of Eqs. (12.a) and (12.b) were compared. According to this case, h_a was set to zero in Eq. (7) and $G_2 = 0$ (that represent $h_a = 0$) was fixed in Eq. (12.b). To generalize the analysis and facilitate the comparison, the position of the "dissolution–diffusion moving front" was transformed into a dimensionless variable using the following relationships: $\delta = (R_e - S)/R_0$, where δ is the dimensionless position of the "dissolution–diffusion moving fronts". The simulation results are presented in Fig. 4a. It can be seen that the theoretical positions of the "dissolution–diffusion moving front" calculated according to Eq. (7) are identical to that predicted by our model previously reported (Helbling et al., 2011). Also, the behavior of the Eqs. (12.a) and (12.b) are indistinguishable, showing that the more complex models behave exactly like the corresponding equations derived for systems without external resistance layer.

In addition, the cumulative amount of solute released was compared. For the one-layer device, the theoretical prediction of Eq. (9) was compared with the model previously reported by Helbling et al. (2011) and for the two-layer device, the behaviors of Eqs. (14.a) and (14.b) were compared. $C_{eq,1} = 0$ in Eq. (9) and $C_{m,2} = 0$ in Eq. (14.b) (that represents $h_a = 0$) were set in accordance with this limit situation. The simulation results are presented in Fig. 4b. The figure shows that Eqs. (9) and (14.b) behave exactly like the corresponding equations derived for systems without external resistance layer.

After checking that the equations behave similarly in the absence of external resistance layer, the next step was to analyze the behavior of the models in absence of the membrane. For this purpose, the positions of the "dissolution–diffusion moving fronts" and the cumulative amount of solute released calculated according to Eqs. (12.a) and (14.a), respectively, were compared with the theoretical predictions of the previously reported model (Helbling

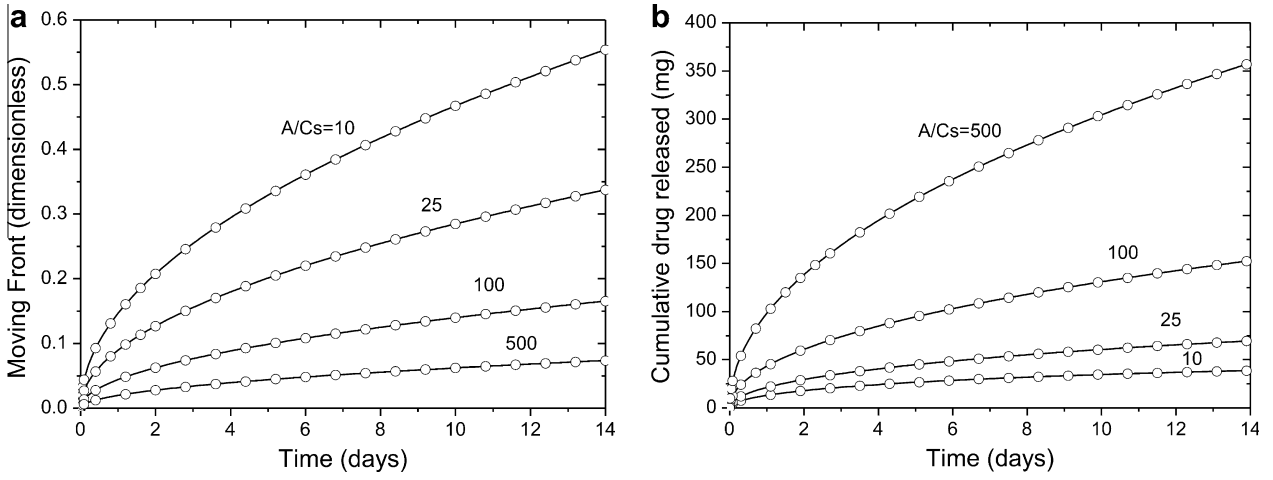

Fig. 5. Comparison of the equations behavior in absence of membrane and external resistance layer for different A/C_s ratios: (a) (—) model reported by Helbling et al. (2011) and (○) Eq. (12.a). (b) (—) model reported by Helbling et al. (2011) and (○) Eq. (14.a). The parameters used are: $C_s = 1$ mg/cm^3; $R_e = 3.15$ cm; $R_g = 2.85$ cm; $R_0 = 0.30$ cm; $D_p = 1 \times 10^{-7}$ cm^2/s; $h_m = 0$; $h_a = 0$.

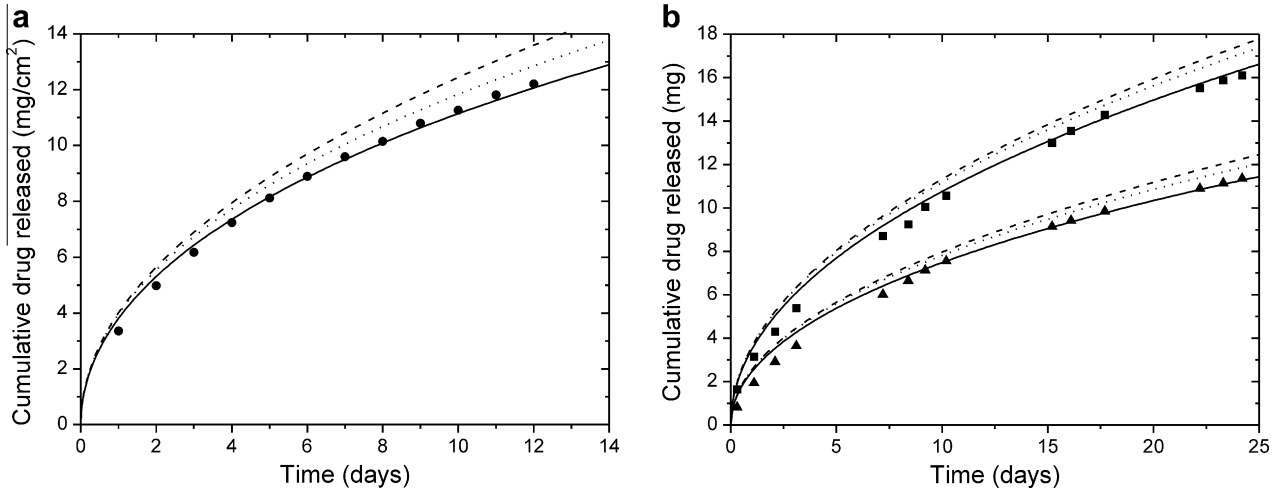

Fig. 6. (a) Comparison of release profiles calculated according to Eq. (9) (—), model reported by Roseman and Higuchi (1970) (···), model reported by Higuchi (1963) (- - -) and the experimental data reported by Chien et al. (●) (Chien et al., 1974), for ethynodiol diacetate release from a silicone device. The parameters used are: AV_s = 647.57 mg; R_e = 3.15 cm; R_g = 2.85 cm; R_0 = 0.30 cm; a_{rel} = 33.75 cm^2; V_s = 5.06 cm^3; C_s = 1.4791 mg/cm^3. (b) Comparison of release profiles calculated according to Eq. (9) (—), model reported by Roseman and Higuchi (1970) (···), model reported by Higuchi (1963) (—) and the experimental data reported by Jackanicz (symbols) (Jackanicz, 1981) for levonorgestrel release from a silicone vaginal ring: (▲) AV_s = 35 mg (■) AV_s = 70 mg. The parameters used are: R_e = 2.85 cm; R_g = 2.43 cm; R_0 = 0.42 cm; V_s = 8.46cm^3; C_s = 0.016 mg/cm^3.

et al., 2011) for different A/C_s ratios. For the comparison, h_m was set to zero in Eq. (12.a) and $C_{eq,2}$ = 0 (that represent h_m = 0) was fixed in Eq. (14.a) according to this limit situation. The simulation results are presented in Fig. 5. It can be seen that Eqs. (12.a) and (14.a) behave exactly like the corresponding equations derived for the one-layer device for all the A/C_s ratios analyzed. It can be concluded that the equations derived for more complex systems (two-layer or with external resistance layer) can reproduce very well the behavior of the simplest model by taking the asymptotic cases of the former.

3.2. Comparisons with experimental release profiles

The second step in the validation process was to verify the ability of the models to predict real experimental drug release profiles. This goal was achieved by comparison of several examples of vaginal rings experimental release profiles reported in the literature with the theoretical results given by the developed models. Since the results in Section 3.1 showed the validity of the models for systems with external resistance layer and due to the difficulty of finding experimental release profiles with all the model parameters known for this situation, only experimental release data from one-layer and two-layer devices without external resistance layer were analyzed.

Fig. 6 presents examples of controlled release of drug from torus-shaped one-layer devices. Fig. 6a shows experimental data reported by Chien et al. for ethynodiol diacetate release from a silicone device (Chien et al., 1974) and the theoretical profiles calculated according to Eq. (9). To obtain the cumulative drug released in the units of mg/cm^2, the result of Eq. (9) was divided by a_{rel}. The parameters employed were taken from Chien et al. (1974) except for the drug diffusion coefficient in the matrix which was found to be $D_p = 5.01 \times 10^{-7}$ cm^2/s from the model adjustment. This value of D_p is in accordance with the value of 10^{-7} cm^2/s reported by Chien et al. (1974). The prediction of the model is in good agreement with the experimental data. Fig. 6b shows experimental data reported by Jackanicz (1981) and the release profiles calculated according to Eq. (9) for levonorgestrel release from silicone vaginal rings with two different initial drug loading. The parameters employed were taken from Jackanicz (1981). The levonorgestrel solubility in the silicone was reported previously by Chien (1982). The diffusion coefficient $D_p = 3.21 \times 10^{-7}$ cm^2/s was obtained from the fitting. It can be seen that the theoretical prediction of the model adjusts the experimental drug release very well. From the Fig. 6 it can be concluded that the model developed for the one-layer device can predict the experimental data very well. Also Fig. 6 presents a comparison of the theoretical predictions of Eq. (9) with the theoretical predictions of reported models developed assuming PSSA for other geometries like cylinder (Roseman and Higuchi, 1970) and sphere (Higuchi, 1963). For the comparison, the cylinders and the spheres have the same dimensions as the torus (for example, the same release area). It can be seen that in all cases the model developed in this work predicts better the drug release profiles from torus-shaped devices than the models developed for other geometries.

Fig. 7 illustrates examples of controlled release of drug from torus-shaped two-layer devices. The figure shows experimental

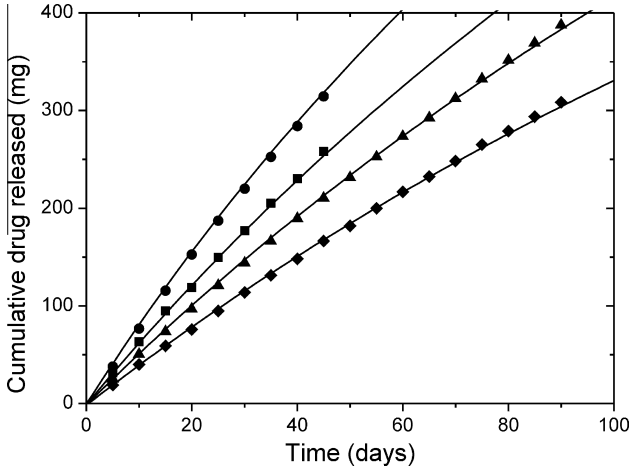

Fig. 7. Comparison of release profiles calculated according to Eq. (14) (—) and the experimental data reported by Matlin et al. (symbols) (Matlin et al., 1992) for progesterone release from silicone vaginal rings: (♦) R_0 = 0.2500 cm; R_e = 2.5250 cm; h_m = 0.2250 cm; (▲) R_0 = 0.3000 cm; R_e = 2.5750 cm; h_m = 0.1750 cm; (■) R_0 = 0.3350 cm; R_e = 2.6100 cm; h_m = 0.1400 cm; (●) R_0 = 0.3625 cm; R_e = 2.6375 cm; h_m = 0.1125 cm. The parameters used are: A/C_s = 475.03; R_g = 2.275 cm; $D_p = D_m$ = 6–8 × 10^{-7} cm^2/s; K_2 = 1.

data reported by Matlin et al. for progesterone release from silicone vaginal rings (Matlin et al., 1992) and the theoretical release profiles calculated according to Eq. (14.a). The experimental devices are composed by two structures: a core of silastic 382 with progesterone dispersed in its interior and a membrane of silastic 382 (not loaded with the hormone) that coats the matrix. The parameters employed were taken from Matlin et al. (1992). The progesterone solubility in the silicone was reported previously by Chien (1982). The diffusion coefficients $D_p = D_m = 6–8 \times 10^{-7}$ cm^2/s were obtained from the fitting and are very close to the value of 10^{-7} cm^2/s reported by Mazan et al. (1993). A close match between the model predictions and the experimental data was observed.

Some methods to compare drug release profiles were proposed in the literature (Costa and Sousa Lobo, 2001; Pillay and Fassihi, 1998). One of the most commonly used is the pair-wise procedure. This procedure includes the *difference factor* and the *similarity factor* proposed originally by Moore and Flanner (1996). The difference factor (f_1) measures the percent error between two curves over all time points while the similarity factor (f_2) is a logarithmic transformation of the sum-squared error of differences between both curves over all time points. The way to calculate these factors has been reported (Costa and Sousa Lobo, 2001; Moore and Flanner, 1996; Pillay and Fassihi, 1998). The Center for Drug Evaluation and Research (FDA) and the Human Medicines Evaluation Unit of the European Agency for the Evaluation of Medicinal Products (EMEA) have been adopted the similarity factor as a criterion for the assessment of the similarity between two in vitro dissolution profiles (Center for Drug Evaluation and Research, 1995; Committee for Proprietary Medicinal Products, 1999). In order to measures quantitatively the fit of the theoretical model to the experimental data, the f_1 and f_2 factors were used. The results given for the release profiles shown in Figs. 6 and 7 are presented in Table 1. The experimental data reported in the literature was selected as the reference product while the model prediction was chosen as the test product. The difference factor is zero when the test and reference profiles are identical and increase proportionally with the dissimilarity between the two profiles (Costa and Sousa Lobo, 2001; Pillay and Fassihi, 1998). The similarity factor is 100 when the test and reference profiles are identical and tends to 0 as the dissimilarity increases. In general, f_1 values lower than 15 (0–15) and f_2 values higher than 50 (50–100) show the similarity of the profiles (Costa and Sousa Lobo, 2001; Pillay and Fassihi, 1998). It can be seen from Table 1 that in all cases the two profiles can be considered similar. Then, it can be concluded that the models predict very well the experimental drug release data reported in the literature for both one-layer and two-layer devices.

Table 1
The *difference* and *similarity* factors for experimental and theoretical drug release profiles comparison.

Reference	Initial amount of drug (mg)	f_1	f_2
a	647.57	2.35	99.28
b	35	3.22	98.95
b	70	2.90	98.75
	R_0 (cm)	f_1	f_2
c	0.2500	1.07	80.69
c	0.3000	1.00	78.30
c	0.3350	1.23	80.87
c	0.3625	2.04	70.50

[a] Chien et al. (1974).
[b] Jackanicz (1981).
[c] Matlin et al. (1992).

3.3. Effect of the thickness of the external resistance layer

In the previous sections the validity of the models has been corroborated. The models are reliable and showed good prediction of experimental release profiles. Once established the validity and reliability of the developed equations, it is important to note the potential that they have. The utility of reliable mathematical models is that previous simulations can be done to optimize a controlled release device. This optimization process involves the study of how different parameters of the models affect the drug release kinetics. In order to illustrate this point, various simulations are presented below.

Fig. 8 illustrates the effect of the thickness of the external resistance layer on the release kinetics from both one-layer and two-layer devices. Fig. 8a corresponds to an one-layer device while Fig. 8b corresponds to a two-layer device. To obtain the fraction of drug released, the result of Eq. (9) or (14) was divided by AV_s, where V_s is the volume of the torus-shaped matrix. The parameter α represents the relative size of h_a with respect to R_0 and is calculated using the following expression:

$$\alpha = 100\frac{h_a}{R_0} \tag{15}$$

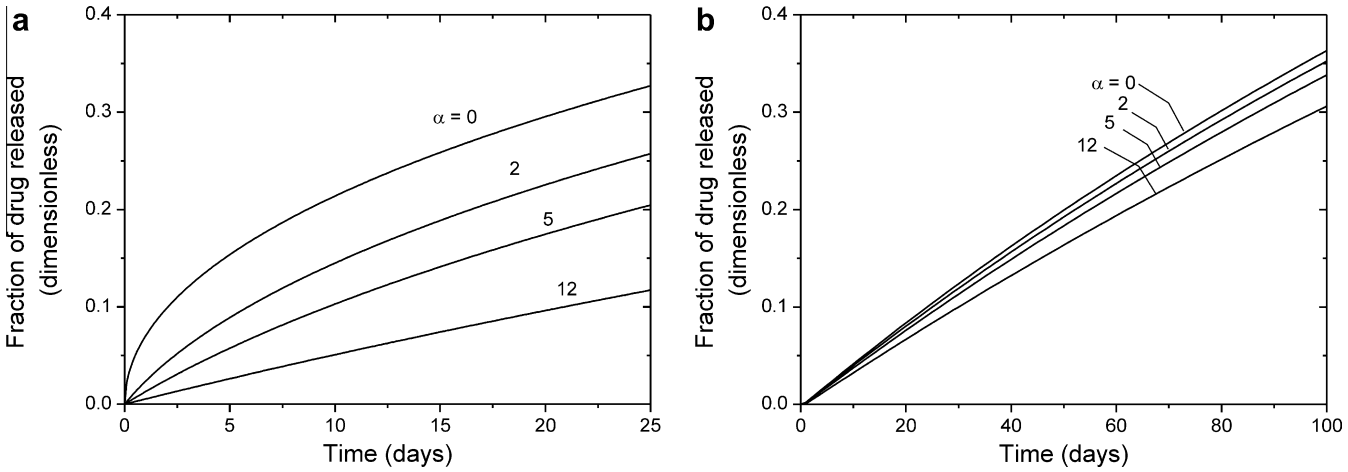

Fig. 8. (a) Comparison of the fraction of drug released calculated according to Eq. (9) for different values of α. The parameters used are: $R_e = 2.85$ cm; $R_g = 2.43$ cm; $R_0 = 0.42$ cm; $AV_s = 35$ mg; $C_s = 0.016$ mg/cm^3; $D_p = D_a = 3.36 \times 10^{-7}$ cm^2/s; $K_1 = 0.5$. (b) Comparison of the fraction of drug released calculated according to Eq. (14) for different values of α. The parameters used are: $R_e = 2.5250$ cm; $R_g = 2.275$ cm; $R_0 = 0.25$ cm; $A = 282.5$ mg/cm^3; $C_s = 0.5947$ mg/cm^3; $D_p = D_m = D_a = 6.5 \times 10^{-7}$ cm^2/s; $K_2 = 1$; $K_3 = 0.5$; $h_m = 0.225$ cm.

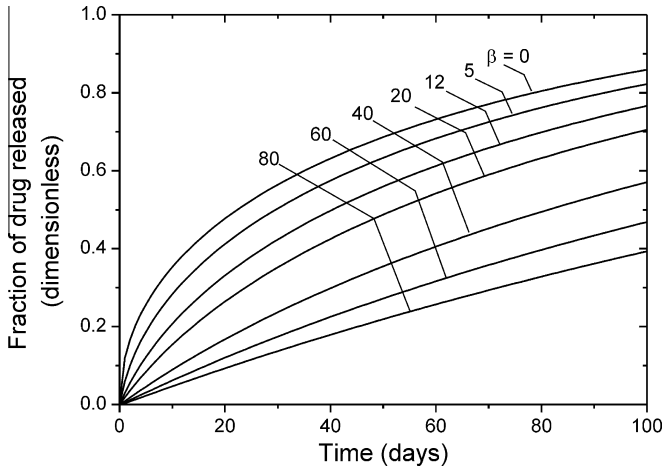

Fig. 9. Comparison of the fraction of drug released calculated according to Eq. (14) for different values of β. The parameters used are: $R_e = 2.5250$ cm; $R_g = 2.275$ cm; $R_0 = 0.25$ cm; $A = 282.5$ mg/cm^3; $C_s = 0.5947$ mg/cm^3; $D_p = D_m = 6.5 \times 10^{-7}$ cm^2/s; $K_2 = 1$; $h_a = 0$ cm.

Fig. 8a shows that with increasing the thickness of the external resistance layer, the drug release decreases. This result is in accordance with those reported by Chien (1982). In addition, it can be observed that increasing the thickness of the external resistance layer, the typical matrix-type profile changes to a straight line. For a two-layer device, also increasing the value of h_a, decreases the release as can be seen in Fig. 8b.

3.4. Effect of the thickness of the second layer

Fig. 9 presents the effect of the thickness of the layer that resembles a membrane (the second layer) on the release kinetics. The parameter β represents the relative size of h_m with respect to R_0 and is calculated as:

$$\beta = 100\frac{h_m}{R_0} \tag{16}$$

It can be seen from the figure that increasing the value of h_m, decreases the fraction of drug released. Also, it can be noted that increasing the thickness of the second layer, the typical matrix-type profile changes to a straight line. This indicates that the release rate is controlled by the membrane and increasing the thickness of the membrane zero-order release kinetics can be reached.

3.5. Effect of the radii of the torus

Fig. 10 presents the effect of the radii of the torus on the release kinetics. Fig. 10a corresponds to a one-layer device while Fig. 10b corresponds to a two-layer device. The parameter γ represents the relative size of R_0 with respect to R_e and is calculated as:

$$\gamma = 100\frac{R_0}{R_e} \tag{17}$$

From Fig. 10a it can be observed that increasing the value of R_0, the release rate diminishes. Alternatively, a decrease in the value of R_e also decreases the release rate. Similar results can be observed in Fig. 10b for a two-layer device.

4. Conclusions

Analytical solutions based on the pseudo-steady state approximation has been successfully derived for both the position of the "dissolution–diffusion moving front" and the cumulative amount of drug released for systems with one-layer and two-layer and having an external mass transfer resistance. The validity of the models was corroborated in two stages. In the first stage, the behavior of the equations derived for more complex systems was compared with the simplest model behavior, taking into account the asymptotic cases of the former. In the second stage, the theoretical predictions of the models were compared with several examples of vaginal rings experimental release data reported in the literature. The simulation results showed that the models derived for more complex systems (two-layer or with external resistance layer) can reproduce very well the behavior of the simplest model by taking the asymptotic cases of the former. In addition, the results showed that the theoretical profiles predicted by the equations are in agreement with the experimental data reported in the literature. The equations can be used easily with the help of an adequate computational software such as MATLAB®. It should be noted however, that the model can be employed only in torus-shaped devices in where the initial drug loading exceeds its solubility in the polymer. In systems where all the solute is dissolved, the model loses its applicability. Also, a simulation study of the effect of the models parameters on release rate was performed. The effects of the thickness of the external resistance layer, the thickness of the second layer and the size of the radii of the torus were analyzed. The obtained results are an illustration of how the drug release kinetics can be adjusted by changing the values of the models parameters. The effect of other parameters like the initial drug loading, diffusion coefficients and partition phenomena can be

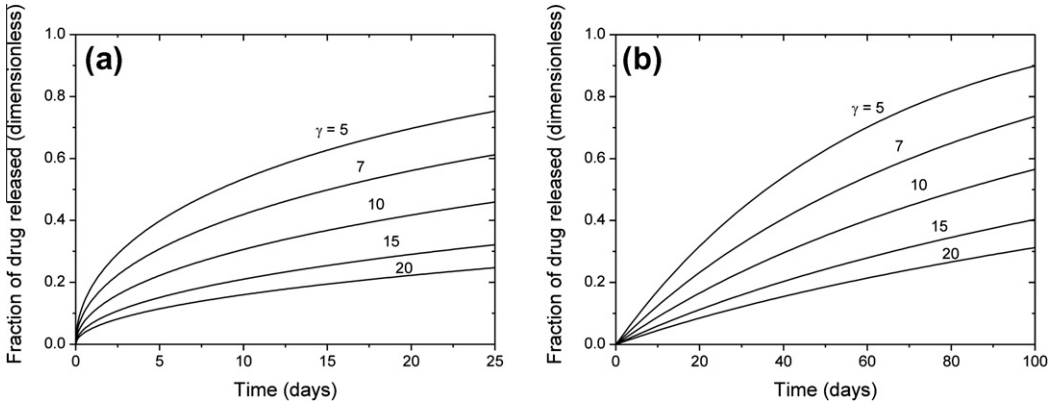

Fig. 10. (a) Comparison of the fraction of drug released calculated according to Eq. (9) for different values of γ. The parameters used are: $R_e = 2.85$ cm; $A = 128$ mg/cm^3; $C_s = 1.4791$ mg/cm^3; $D_p = 3.36 \times 10^{-7}$ cm^2/s; $h_m = 0$ cm; $h_a = 0$ cm. (b) Comparison of the fraction of drug released calculated according to Eq. (14) for different values of γ. The parameters used are: $R_e = 2.5250$ cm; $A = 282.5$ mg/cm^3; $C_s = 0.5947$ mg/cm^3; $D_p = D_m = 6.5 \times 10^{-7}$ cm^2/s; $K_2 = 1$; $h_m = 0.10$ cm; $h_a = 0$ cm.

easily study with the use of the equations derived in this work. The models are an essential tool not only for manufacturing but also for the optimization of torus-shaped controlled release devices.

Acknowledgments

The authors wish to express their gratitude to Consejo Nacional de Investigaciones Científicas y Técnicas (CONICET), and to Universidad Nacional del Litoral (UNL) of Argentina, for the financial support granted to this contribution.

Appendix A

The governing equation for diffusion in the external resistance layer is:

$$\frac{\partial C_{bl}}{\partial t} = \frac{D_a}{r(R_g+r)}\frac{\partial}{\partial r}\left(r(R_g+r)\frac{\partial C_{bl}}{\partial r}\right) \quad t>0 \quad R_e \leqslant r \leqslant R_e + h_a \tag{A.1}$$

The initial and boundary conditions are:

$$C_{bl} = 0 \quad t = 0 \quad R_e \leqslant r \leqslant R_e + h_a \tag{A.2}$$

$$C_{bl} = C_{a,1} \quad t > 0 \quad r = R_e \tag{A.3}$$

$$C_{bl} = 0 \quad t > 0 \quad r = R_e + h_a \tag{A.4}$$

With $\partial C_{bl}/\partial t$ in Eq. (A.1) being fixed at zero according to the PSSA and with the boundary conditions in Eqs. (A.2)–(A.4), the concentration distribution of dissolved-drug in the external resistance layer can be derived as:

$$C_{bl} = K_1 C_{eq,1}\left[1 - \frac{\ln\left(\frac{(R_g+R_e)r}{R_e(R_g+r)}\right)}{\ln\left(\frac{(R_g+R_e)(R_e+h_a)}{R_e(R_g+R_e+h_a)}\right)}\right] \quad t>0 \quad R_e \leqslant r \leqslant R_e + h_a \tag{A.5}$$

where K_1 is the drug partition coefficient at the matrix-external resistance layer interface, which is defined by:

$$K_1 = \frac{C_{a,1}}{C_{eq,1}} \tag{A.6}$$

According to Fick's laws and with the PSSA simplification, at the matrix-external resistance layer interface the following mass balance must be satisfied:

$$\frac{\partial Q}{\partial t} = -D_p\frac{\partial C_t}{\partial r} = -D_a\frac{\partial C_{bl}}{\partial r} \tag{A.7}$$

where Q is the cumulative amount of drug released per unit area of the device. Substituting Eq. (5) and Eq. (A.5) into Eq. (A.7), differentiating with respect to the spatial coordinates and solving for $C_{eq,1}$, the following expression can be achieved:

$$C_{eq,1} = \frac{C_s G_1}{\left(G_1 + \frac{D_a K_1}{D_p}\right)} \tag{A.8}$$

where

$$G_1 = \frac{\ln\left(\frac{(R_g+R_e)(R_e+h_a)}{R_e(R_g+R_e+h_a)}\right)}{\ln\left(\frac{(R_g+S)R_e}{S(R_g+R_e)}\right)} \tag{A.9}$$

Thus, with the expressions of Eqs. (A.8) and (A.9), Eq. (5) can be used.

Appendix B

The governing equation for diffusion in the membrane and the associated initial and boundary conditions are:

$$\frac{\partial C_m}{\partial t} = \frac{D_m}{r(R_g+r)}\frac{\partial}{\partial r}\left(r(R_g+r)\frac{\partial C_m}{\partial r}\right) \quad t>0 \quad R_e \leqslant r \leqslant R_e + h_m \tag{B.1}$$

$$C_m = 0 \quad t = 0 \quad R_e \leqslant r \leqslant R_e + h_m \tag{B.2}$$

$$C_m = C_{m,1} \quad t > 0 \quad r = R_e \tag{B.3}$$

$$C_m = 0 \quad t > 0 \quad r = R_e + h_m \tag{B.4a}$$

$$C_m = C_{m,2} \quad t > 0 \quad r = R_e + h_m \tag{B.4b}$$

The boundary condition in the external surface of the two-layer device is represented by Eq. (B.4) and varies depending on which system is considered. The Eq. (B.4a) corresponds to the system without external resistance illustrated in Fig. 3a and the Eq. (B.4b) corresponds to the system that has an external resistance layer shown in Fig. 3b. This nomenclature is used throughout this section: the equations with subscript "a" in the equations number correspond to the system without external resistance layer illustrated in Fig. 3a while those having subscript "b" correspond to the system with external resistance layer illustrated in Fig. 3b. With $\partial C_m/\partial t$ in Eq. (B.1) being fixed at zero according to the PSSA and with the conditions in Eqs. (B.2)–(B.4), the concentration distribution of dissolved-drug in the membrane can be derived as:

$$C_m = K_2 C_{eq,2}\left[1 - \frac{\ln\left(\frac{(R_g+R_e)r}{R_e(R_g+r)}\right)}{\ln\left(\frac{(R_g+R_e)(R_e+h_m)}{R_e(R_g+R_e+h_m)}\right)}\right] \quad t>0 \quad R_e \leqslant r \leqslant R_e + h_m \tag{B.5a}$$

$$C_m = K_2 C_{eq,2}\left[1 - \frac{\ln\left(\frac{(R_g+R_e)r}{R_e(R_g+r)}\right)}{\ln\left(\frac{(R_g+R_e)(R_e+h_m)}{R_e(R_g+R_e+h_m)}\right)}\right] + C_{m,2}\frac{\ln\left(\frac{(R_g+R_e)r}{R_e(R_g+r)}\right)}{\ln\left(\frac{(R_g+R_e)(R_e+h_m)}{R_e(R_g+R_e+h_m)}\right)} \quad t>0 \quad R_e \leqslant r \leqslant R_e + h_m \tag{B.5b}$$

where K_2 is the drug partition coefficient at the matrix-membrane interface, which is defined by:

$$K_2 = \frac{C_{m,1}}{C_{eq,2}} \tag{B.6}$$

The Eq. (B.5a) can be employed to establish the expression of $C_{eq,2}$ but for the use of Eq. (B.5b) for this purpose, the expression of $C_{m,2}$ must be determined first. This goal can be done as in Appendix A. The concentration distribution of dissolved-drug in the external resistance layer can be derived using Eqs. (A.1)–(A.4), except that in this case the domain is $R_e + h_m \leqslant r \leqslant R_e + h_m + h_a$ and the condition in Eq. (A.3) is replaced by $C_{bl} = C_{a,2}$ for $t > 0$ and $r = R_e + h_m$. According to Fick's laws and with the PSSA simplification, at the membrane-external resistance layer interface the following mass balance must be satisfied:

$$\frac{\partial Q}{\partial t} = -D_m\frac{\partial C_m}{\partial r} = -D_a\frac{\partial C_{bl}}{\partial r} \tag{B.7}$$

Substituting Eq. (B.5b) and the expression of C_{bl} (not shown) into Eq. (B.7), differentiating with respect to the spatial coordinates and solving for $C_{m,2}$, the following expression can be achieved:

$$C_{m,2} = \frac{D_m K_2 G_2 C_{eq,2}}{(D_m G_2 + D_a K_3)} \tag{B.8}$$

where

$$G_2 = \frac{\ln\left(\frac{(R_g+R_e+h_m)(R_e+h_m+h_a)}{(R_e+h_m)(R_g+R_e+h_m+h_a)}\right)}{\ln\left(\frac{(R_g+R_e)(R_e+h_m)}{R_e(R_g+R_e+h_m)}\right)} \tag{B.9}$$

and K_3 is the drug partition coefficient at the membrane-external resistance layer interface, which is defined by:

$$K_3 = \frac{C_{a,2}}{C_{m,2}} \tag{B.10}$$

Thus, with the expressions of Eqs. (B.8) and (B.9), Eq. (B.5b) can be used. At the matrix-membrane interface, the following mass balance equation must be satisfied:

$$\frac{\partial Q}{\partial t} = -D_p \frac{\partial C_t}{\partial r} = -D_m \frac{\partial C_m}{\partial r} \tag{B.11}$$

Substituting Eq. (11) and Eq. (B.5a) or (B.5b) into Eq. (B.11), differentiating with respect to the spatial coordinates and solving for $C_{eq,2}$, the following expressions can be achieved:

$$C_{eq,2} = \frac{C_s G_3}{\left(G_3 + \frac{D_m K_2}{D_p}\right)} \tag{B.12a}$$

$$C_{eq,2} = \frac{C_s G_3}{\left(G_3 + \frac{D_m K_2}{D_p} - \frac{D_m^2 K_2 G_2}{D_p (D_m G_2 + D_a K_3)}\right)} \tag{B.12b}$$

where

$$G_3 = \frac{\ln\left(\frac{(R_g+R_e)(R_e+h_m)}{R_e(R_g+R_e+h_m)}\right)}{\ln\left(\frac{(R_g+S)R_e}{S(R_g+R_e)}\right)} \tag{B.13}$$

Therefore, with the expressions of $C_{eq,2}$ given by Eqs. (B.12a) and (B.12b), the Eq. (11) can be employed.

References

Arifin, D.Y., Lee, L.Y., Wang, C.H., 2006. Mathematical modeling and simulation of drug release from microspheres: implications to drug delivery systems. Adv. Drug Deliv. Rev. 58, 1274–1325.

Center for Drug Evaluation, Research, 1995. Food and Drug Administration. Guidance for Industry: Immediate Release Solid Oral Dosage Forms. Scale-Up and Postapproval Changes: Chemistry, Manufacturing, and Controls, In Vitro Dissolution Testing, and In Vivo BE Documentation. US Department of Health and Human Services, Food and Drug Administration, Rockville, MD.

Chien, Y.W., 1982. Fundamentals of controlled-release drug administration. In: Swarbrick, J. (Ed.), Novel Drug Delivery System. Marcel Dekker Inc., New York and Basel, pp. 465–574.

Chien, Y.W., Lambert, H.J., Grant, D.E., 1974. Controlled drug release from polymeric devices. I. Technique for rapid in vitro release studies. J. Pharm. Sci. 63, 365–369.

Cicinelli, E., 2008. Intravaginal oestrogen and progestin administration: advantages and disadvantages. Best Pract. Res. Clin. Obstet. Gynaecol. 22, 391–405.

Committee for Proprietary Medicinal Products, 1999. Note for Guidance on Quality of Modified Release Products: A: Oral Dosage Forms, B: Transdermal Dosage Forms. Section I (Quality). CPMP/QWP/604/96. London, England.

Costa, P., Sousa Lobo, J.M., 2001. Modeling and comparison of dissolution profiles. Eur. J. Pharm. Sci. 13, 123–133.

Costa, P., Sousa Lobo, J.M., 2003. Evaluation of mathematical models describing dug release from estradiol transdermal systems. Drug Dev. Ind. Pharm. 29, 89–97.

Crank, J., 1975. The Mathematics of Diffusion, second ed. Clarendon Press, Oxford.

Fick, A., 1855. Ueber diffusion. Ann. Phys. 170, 59–86.

Helbling, I.M., Ibarra, J.C.D., Luna, J.A., Cabrera, M.I., Grau, R.J.A., 2010a. Modeling of dispersed-drug delivery from planar polymeric systems: optimizing analytical solutions. Int. J. Pharm. 400, 131–137.

Helbling, I.M., Ibarra, J.C.D., Luna, J.A., Cabrera, M.I., Grau, R.J.A., 2010b. Modeling of drug delivery from erodible and non-erodible laminated planar devices into a finite external medium. J. Membr. Sci. 350, 10–18.

Helbling, I.M., Luna, J.A., Cabrera, M.I., 2011. Mathematical modeling of drug delivery from torus-shaped single-layer devices. J. Control. Release 149, 258–263.

Higuchi, T., 1961. Rate of release of medicaments from ointment bases containing drug in suspension. J. Pharm. Sci. 50, 874–875.

Higuchi, T., 1963. Mechanism of sustained-action medication. J. Pharm. Sci. 52, 1145–1149.

Hussain, A., Ahsan, F., 2005. The vagina as a route for systemic drug delivery. J. Control. Release 103, 301–313.

Jackanicz, T.M., 1981. Levonorgestrel and estradiol release from an improved contraceptive vaginal ring. Contraception 24, 323–339.

Johansson, E.D.B., Sitruk-Ware, R., 2004. New delivery systems in contraception: vaginal rings. Am. J. Obstet. Gynecol. 190, S54–S59.

Malcolm, R.K., McCullagh, S., Woolfson, A.D., Catney, M., Tallon, P., 2002. A dynamic mechanical method for determining the silicone elastomer solubility of drug and pharmaceutical excipients in silicone intravaginal drug delivery rings. Biomaterials 23, 3589–3594.

Malcolm, R.K., Woolfson, A.D., Russell, J., Andrews, C., 2003a. In vitro release of nonoxynol-9 from silicone matrix intravaginal rings. J. Control. Release 91, 355–364.

Malcolm, R.K., Woolfson, A.D., Russell, J., Tallon, P., McAuley, L., Craig, D., 2003b. Influence of silicone elastomer solubility and diffusivity on the in vitro release of drugs from intravaginal rings. J. Control. Release 90, 217–225.

Matlin, S.A., Belenguer, A., Hall, P.E., 1992. Progesterone-releasing vaginal rings for use in postpartum contraception. I. In vitro release rates of progesterone from core-loaded rings. Contraception 45, 329–341.

Mazan, J., Leclerc, B., Porte, H., Torres, G., Couarraze, G., 1993. Influence of network characteristics on diffusion in silicone elastomer. J. Mater. Sci. Mater. Med. 4, 175–178.

Moore, J.W., Flanner, H.H., 1996. Mathematical comparison of dissolution profiles. Pharm. Tech. 20, 64–74.

Özişik, M.N., 1980. Heat Conduction. John Wiley & Sons Inc., New York.

Pillay, V., Fassihi, R., 1998. Evaluation and comparison of dissolution data derived from different modified release dosage forms: an alternative method. J. Control. Release 55, 45–55.

Roseman, T.J., 1972. Release of steroids from a silicone polymer. J. Pharm. Sci. 61, 46–50.

Roseman, T.J., Higuchi, W.I., 1970. Release of medroxyprogesterone acetate from a silicone polymer. J. Pharm. Sci. 59, 353–357.

Roumen, F.J.M.E., 2008. Review of the combined contraceptive vaginal ring, NuvaRing®. Ther. Clin. Risk Manag. 4, 441–451.

Siepmann, F., Herrmann, S., Winter, G., Siepmann, J., 2008. A novel mathematical model quantifying drug release from lipid implants. J. Control. Release 128, 233–240.

Siepmann, J., Siepmann, F., 2008. Mathematical modeling of drug delivery. Int. J. Pharm. 364, 328–343.

Sitruk-Ware, R., 2006. Contraception: an international perspective. Contraception 73, 215–222.

Tojo, K., 1985. Intrinsic release rate from matrix-type drug delivery systems. J. Pharm. Sci. 74, 685–687.

Van Laarhoven, J.A.H., Kruft, M.A.B., Vromans, H., 2002. In vitro release properties of levonorgestrel and ethinyl estradiol from a contraceptive vaginal ring. Int. J. Pharm. 232, 163–173.

Woolfson, A.D., Elliott, G.R.E., Gilligan, C.A., Passmore, C.M., 1999. Design of an intravaginal ring for the controlled delivery of 17β-estradiol as its 3-acetate ester. J. Control. Release 61, 319–328.

Woolfson, A.D., Malcolm, R.K., Gallagher, R.J., 2003. Design of a silicone reservoir intravaginal ring for the delivery of oxybutynin. J. Control. Release 91, 465–476.

Wu, L., Brazel, C.S., 2008. Mathematical model to predict drug release, including the early-time burst effect, from swellable homogeneous hydrogels. Ind. Eng. Chem. Res. 47, 1518–1526.

Yoo, J., Lee, C.H., 2006. Drug delivery systems for hormone therapy. J. Control. Release 112, 1–14.

Zhou, Y., Wu, X.Y., 2002. Theoretical analyses of dispersed-drug release from planar matrices with a boundary layer in a finite medium. J. Control. Release 84, 1–13.

Zhou, Y., Wu, X.Y., 2003. Modeling and analysis of dispersed-drug release into a finite medium from sphere ensembles with a boundary layer. J. Control. Release 90, 23–36.